



## Synthesis of new bipolar host materials based on 1,2,4-oxadiazole for blue phosphorescent OLEDs



Qian Li<sup>a</sup>, Lin-Song Cui<sup>a</sup>, Cheng Zhong<sup>b,\*\*\*</sup>, Xiao-Dong Yuan<sup>a</sup>, Shou-Cheng Dong<sup>a</sup>, Zuo-Quan Jiang<sup>a,\*</sup>, Liang-Sheng Liao<sup>a,\*\*</sup>

<sup>a</sup>Jiangsu Key Laboratory for Carbon-Based Functional Materials & Devices, Institute of Functional Nano & Soft Materials (FUNSOM), Soochow University, Suzhou, Jiangsu 215123, China

<sup>b</sup>Department of Chemistry, Hubei Key Lab on Organic and Polymeric Optoelectronic Materials, Wuhan University, Wuhan 430072, China

### ARTICLE INFO

#### Article history:

Received 20 August 2013

Received in revised form

13 September 2013

Accepted 16 September 2013

Available online 4 October 2013

#### Keywords:

OLEDs

1,2,4-Oxadiazole

Bipolar

Host material

Electrophosphorescence

High triplet energy

### ABSTRACT

Two novel bipolar host materials, namely 3,5-bis(4-(9H-carbazol-9-yl)phenyl)-1,2,4-oxadiazole (**pCzmOXD**) and 3,5-bis(3-(9H-carbazol-9-yl)phenyl)-1,2,4-oxadiazole (**mCzmOXD**) were designed and synthesized, by incorporating a new block 1,2,4-oxadiazole as the n-type moiety and changing its linking pattern with carbazole. As expected, high triplet energy (over 2.81 eV) for **mCzmOXD** was achieved due to the intrinsic *meta*-linkage of 1,2,4-oxadiazole. When both materials were applied in blue phosphorescent organic light-emitting diodes, good performance of 13.0 cd A<sup>-1</sup>/16.0 cd A<sup>-1</sup> were achieved for **pCzmOXD** and **mCzmOXD** in iridium(III) bis[(4,6-difluorophenyl)pyridinato-N, C<sup>2'</sup>] picolinate (Flrpic)-based devices, respectively.

Crown Copyright © 2013 Published by Elsevier Ltd. All rights reserved.

### 1. Introduction

There are four different regioisomeric forms of the classic five-membered heterocycles oxadiazoles, namely 1,2,5-oxadiazole, 1,3,4-oxadiazole, 1,2,4-oxadiazole and 1,2,3-oxadiazole. Their derivatives have attracted a wide attention of chemist in searching for the new therapeutic molecules and in developing new optoelectronic materials especially with the rise of organic semiconductors. That is mainly because of their electron-deficient nature which is suitable for designing n-type semiconductor in material research [1–4]. Among the four oxadiazoles (Scheme 1), the 1,2,3-isomer is unstable and easily reverts to the diazoketone tautomer [5]; the 1,2,5-isomer incorporating with one phenyl ring to form 2,1,3-benzooxadiazole and 1,3,4-isomer appending with two phenyl rings to form diphenyl-1,3,4-oxadiazole are two common blocks in synthesizing optoelectronic materials, which could be used in

polymeric solar cells (PSCs) [6–9] and organic light-emitting diodes (OLEDs) [10–14].

In comparison with the 1,2,5-isomer and 1,3,4-isomer, the 1,2,4-oxadiazole has received very little attention in the study of optoelectronics. By analyzing the structure difference of these three isomers, we found that they correspond well with three kinds of conjugation modes-*ortho*, *meta* and *para* in substitution (Scheme 1). Similar theoretical studies on *meta*-linked phenylene compounds suggest that these groups interrupt the conjugation by introducing kinks into the backbone which will lead to a helical conformation [15]. Accordingly, the introduction of *meta*-linkages could also influence both the electron delocalization and the conjugation degree of oxadiazole-based derivatives. Thus, the *meta*-linkage, e.g. the derivation based on 1,2,4-oxadiazole, will result in the highest S<sub>1</sub> and T<sub>1</sub> energies among the isomers [16–18].

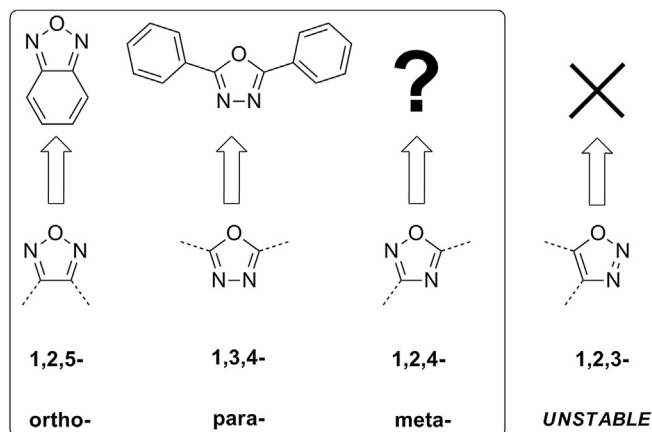
This merit could be utilized in designing high triplet energy host materials in phosphorescent OLEDs (PHOLEDs) [19–22]. It is well known that the PHOLEDs could achieve 100% internal external efficiency by harvesting both the singlet/triplet excitons in device and have made significant progress in the past decade [23]. This progress is closely related to the development of host materials, which is used to disperse the phosphor emitter's concentration to deter the triplet–triplet annihilation or triplet–polaron annihilation [24].

\* Corresponding author. Tel.: +86 521 65880093; fax: +86 521 658808220.

\*\* Corresponding author. Tel.: +86 521 65880945; fax: +86 521 658808220.

\*\*\* Corresponding author. Tel.: +86 27 68752330; fax: +86 27 68756757.

E-mail addresses: [zhongcheng@whu.edu.cn](mailto:zhongcheng@whu.edu.cn) (C. Zhong), [zqjiang@suda.edu.cn](mailto:zqjiang@suda.edu.cn) (Z.-Q. Jiang), [lslliao@suda.edu.cn](mailto:lslliao@suda.edu.cn) (L.-S. Liao).



Scheme 1. Four different regioisomeric forms of oxadiazole.

The first principle of host materials is that the triplet energy of host must be higher than that of guest [25–27]. This requirement is critical for high device efficiency by confine the excitons in the emitting layer. Another issue to achieve high efficiency is balancing the carrier transport and thus broadening the combination zone. For this purpose, the concept of bipolar host materials was proposed and the 1,3,4-oxadiazole bearing the electron-transport property had played a major role in this topic. For example, Yang's group have synthesized a series of bipolar host materials based on 1,3,4-oxadiazole and achieved good results in green and red emission [28–30]. However, there is still a dilemma between pursuing high triplet energy and reducing the interplay from hole-transport moiety to electron-transport moiety, especially for the most important blue phosphorescence [31,32]. That is because a strong donor–acceptor (D–A) interaction will lower the  $T_1$  state, owing to the formation of intramolecular charge-transfer (CT) states [33]. There are two alternatives for this quandary: interrupting the conjugation between hole-transport/electron-transport moieties by insulating linkage, such as  $sp^3$  hybridized Si or C atoms, or developing new blocks with higher triplet energies.

Thus in this article, we firstly utilized 1,2,4-oxadiazole as the electron-withdrawing group in the design and synthesis of bipolar host materials. 3,5-bis(4-(9H-carbazol-9-yl)phenyl)-1,2,4-oxadiazole (**pCzmOXD**) and 3,5-bis(3-(9H-carbazol-9-yl)phenyl)-1,2,4-oxadiazole (**mCzmOXD**) were prepared and their thermal, photophysical, and electrochemical properties were fully investigated. The two materials were used as host materials of blue phosphorescent OLEDs and the device performances were evaluated. When **pCzmOXD** and **mCzmOXD** were employed as the host for the phosphor iridium(III) bis[(4,6-difluorophenyl)pyridinato-N, C<sup>2'</sup>] picolinate (Flrpic) in PHOLEDs, current efficiencies of 13.0 and 16.0  $\text{cd A}^{-1}$ , with external quantum efficiencies of 5.6% and 6.8%, were achieved.

## 2. Experimental

### 2.1. Chemicals and instruments

All chemicals purchased were used without further purification, and intermediates were purified and dried before using. Solvents used in the synthetic routes were purified by PURE SOLV (Innovative Technology) purification system. All the other reagents were used as received from commercial sources.

$^1\text{H}$  NMR and  $^{13}\text{C}$  NMR spectra were measured on a Varian Unity Inova 400 spectrometer at room temperature, and the chemical shifts were quoted relative to  $\text{SiMe}_4$ . Mass spectra were recorded on

a Thermo ISQ mass spectrometer using a direct exposure probe. UV–Vis absorption spectra were obtained by a Perkin Elmer Lambda 750 spectrophotometer. Photoluminescence (PL) spectra and phosphorescent spectra were recorded on a Hitachi F-4600 fluorescence spectrophotometer. For thermal properties, differential scanning calorimetry (DSC) was performed on a TA DSC 2010 unit at a heating rate of  $10\text{ }^\circ\text{C}/\text{min}$  under a nitrogen atmosphere to determine the glass transition temperatures ( $T_g$ ) from the second heating scan.

Electrochemical measurements were made using a CHI600 voltammetric analyzer. A conventional three-electrode configuration consisting of a platinum working electrode, a Pt-wire counter electrode, and an Ag/AgCl reference electrode was used. The solvent in all measurements was  $\text{CH}_2\text{Cl}_2$ , and the supporting electrolyte was 0.1 M  $[\text{Bu}_4\text{N}]\text{PF}_6$ . Ferrocene was added as a calibrant after each set of measurements, and all potentials reported were quoted with reference to the ferrocene–ferrocenium ( $\text{Fc}/\text{Fc}^+$ ) couple at a scan rate of  $100\text{ mV s}^{-1}$ . Theoretical calculations based on density functional theory (DFT) approach at the B3LYP level were performed with the use of Gaussian 09 program.

### 2.2. General procedures for the preparation of **pCzmOXD** and **mCzmOXD**

#### 2.2.1. Preparation of 3,5-bis(4-fluorophenyl)-1,2,4-oxadiazole (**pFmOXD**)

4-Fluorobenzonitrile (3.33 g, 27.47 mmol), hydroxylamine hydrochloride (4.20 g, 60.44 mmol) and triethylamine (6.40 g, 8.77 ml, 63.37 mmol) were dissolved by 40 ml ethanol and 2 ml water in a 100 ml flask, then the mixture was heated to  $75\text{ }^\circ\text{C}$  for 12 h. After cooled to room temperature added 65 ml water in the solution, then evaporated the ethanol in the solution with a rotary evaporator to get white powder precipitated out. Dried the white powder 4-fluoro-N'-hydroxybenzimidamide after filtered, then they can be used directly in the next step.

4-fluorobenzoic acid (2.80 g, 20.0 mmol) and sulfurous dichloride (4.76 g, 2.92 ml, 40.0 mmol) were added in a 100 ml flask, then the mixture was stirred at room temperature for 10 min,  $76\text{ }^\circ\text{C}$  refluxed for 30 min, stirred at  $80\text{ }^\circ\text{C}$  for 3 h. Redundant sulfurous dichloride was removed by reduced pressure distillation, then 4-fluorobenzoyl chloride was achieved. Then 4-fluoro-N'-hydroxybenzimidamide (3.00 g, 19.46 mmol) afforded before and 20 ml DMF were added into the flask, and heated to  $120\text{ }^\circ\text{C}$  stirred for 30 min. After cooling to room temperature, the reaction mixture was dumped into ice water and filtered, washed with water. The crude material was purified by column chromatography with 1:3 (v/v) dichloromethane/petroleum ether as the eluent to give a white solid (4.29 g).

83.2% yield.  $^1\text{H}$  NMR (400 MHz,  $\text{CDCl}_3$ )  $\delta$  (ppm): 8.23–8.21(m, 2H), 8.19–8.15(m, 2H), 7.27–7.18(m, 4H).  $^{13}\text{C}$  NMR ( $\text{CDCl}_3$ )  $\delta$  (ppm): 174.91, 168.21, 166.81, 165.91, 164.27, 163.41, 132.87, 130.68, 130.59, 129.74, 129.65, 123.08, 120.62, 116.43, 116.19, 115.97, 115.61. MS (EI):  $m/z$  258.29 [ $\text{M}^+$ ]. Anal. calcd for  $\text{C}_{14}\text{H}_8\text{F}_2\text{N}_2\text{O}$  (%): C 65.12, H 3.12, N 10.85; found: C 64.32, H 3.23, N 10.39.

#### 2.2.2. Preparation of 3,5-bis(3-bromophenyl)-1,2,4-oxadiazole (**mBrmOXD**)

**mBrmOXD** was synthesized according to the same procedure as for **pFmOXD** by using 3-bromobenzonitrile (5.00 g, 27.47 mmol) and 3-bromobenzoic acid (4.02 g, 20.0 mmol). **mBrmOXD** (6.42 g) was afforded as a white solid.

84.5% yield.  $^1\text{H}$  NMR (400 MHz,  $\text{CDCl}_3$ )  $\delta$  (ppm): 8.39–8.33 (m, 2H), 8.16–8.14 (d,  $J = 8.0\text{ Hz}$ , 1H), 8.12–8.10 (d,  $J = 8.0\text{ Hz}$ , 1H), 7.75–7.65 (m, 2H), 7.47–7.38 (m, 2H).  $^{13}\text{C}$  NMR ( $\text{CDCl}_3$ )  $\delta$  (ppm): 174.64, 167.99, 135.90, 134.34, 131.11, 130.74, 130.56, 130.48, 128.65, 126.68,

126.05, 125.88, 123.23, 123.01. MS (EI):  $m/z$  380.15 [ $M^+$ ]. Anal. calcd for  $C_{14}H_8Br_2N_2O$  (%): C 44.25, H 2.12, N 7.37; found: C 44.26, H 2.03, N 7.20.

### 2.2.3. Preparation of 3,5-bis(4-(9H-carbazol-9-yl)phenyl)-1,2,4-oxadiazole (**pCzmOXD**)

**pFmOXD** (2.58 g, 10.00 mmol), carbazole (5.01 g, 30.00 mmol) and  $K_2CO_3$  (8.28 g, 60.00 mmol) were dissolved in 30 ml DMSO. The reaction mixture was heated to 150 °C for 12 h under an argon atmosphere. After cooling to room temperature, the mixture was dumped into ice water and filtered, washed with water. The crude material was purified by column chromatography with 1:3 (v/v) dichloromethane/petroleum ether as the eluent to give a white solid (4.48 g).

81.2% yield.  $^1H$  NMR (400 MHz,  $CDCl_3$ )  $\delta$  (ppm): 8.52–8.50 (d,  $J = 8.8$  Hz, 2H), 8.48–8.46 (d,  $J = 8.4$  Hz, 2H), 8.18–8.16 (d,  $J = 8.0$  Hz, 4H), 7.86–7.84 (d,  $J = 8.4$  Hz, 2H), 7.80–7.77 (d,  $J = 8.4$  Hz, 2H), 7.55–7.51 (t, 4H), 7.48–7.44 (m, 4H), 7.37–7.31 (m, 4H).  $^{13}C$  NMR ( $CDCl_3$ )  $\delta$  (ppm): 142.10, 140.55, 140.48, 140.19, 129.98, 129.24, 127.23, 126.32, 126.18, 125.66, 123.95, 123.73, 122.62, 120.78, 120.56, 120.46, 120.43. MS (EI):  $m/z$  552.56 [ $M^+$ ]. Anal. calcd for  $C_{38}H_{24}N_4O$  (%): C 82.59, H 4.38, N 10.14; found: C 82.04, H 4.47, N 10.14.

### 2.2.4. Preparation of 3,5-bis(3-(9H-carbazol-9-yl)phenyl)-1,2,4-oxadiazole (**mCzmOXD**)

**mBrmOXD** (3.80 g, 10.00 mmol), carbazole (5.01 g, 30.00 mmol) dissolved in anhydrous xylene (60 ml) under an argon atmosphere. Sodium *tert*-butoxide, *S*-PHOS and tris(dibenzylideneacetone)

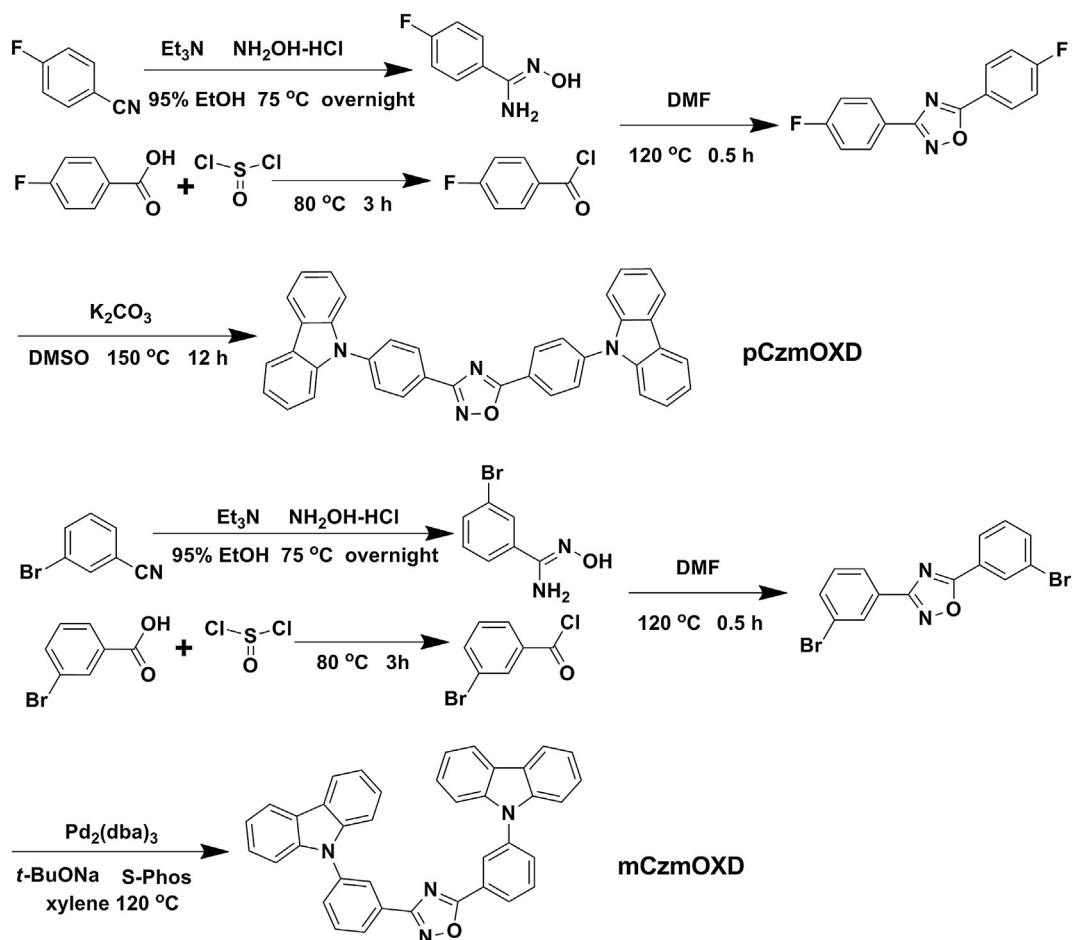
dipalladium (0) were added to the reaction mixture. The mixture was stirred at 110 °C for 48 h. After the reaction was finished, the organic layer was separated and washed with dichloromethane and water, then the organic layer was dried over by anhydrous  $Na_2SO_4$ , filtered and evaporated under reduced pressure. The crude material was purified by column chromatography with 1:3 (v/v) dichloromethane/petroleum ether as the eluent to give a white solid state **mCzmOXD** (3.85 g).

69.7% yield.  $^1H$  NMR (400 MHz,  $CDCl_3$ )  $\delta$  (ppm): 8.44–8.41 (d,  $J = 14.4$  Hz, 2H), 8.29–8.25 (m, 2H), 8.16–8.14 (d,  $J = 8.0$  Hz, 2H), 7.83–7.73 (m, 4H), 7.46–7.39 (m, 8H), 7.32–7.27 (m, 4H).  $^{13}C$  NMR ( $CDCl_3$ )  $\delta$  (ppm): 175.19, 168.56, 140.70, 140.53, 138.85, 138.50, 131.35, 130.89, 130.55, 129.87, 129.74, 129.38, 128.74, 126.91, 126.64, 126.40, 126.22, 126.10, 125.99, 123.64, 123.53, 120.46, 120.37, 120.20. MS (EI):  $m/z$  552.51 [ $M^+$ ]. Anal. calcd for  $C_{38}H_{24}N_4O$  (%): C 82.59, H 4.38, N 10.14; found: C 82.58, H 4.37, N 10.23.

### 2.3. Device fabrication and characterization

PHOLEDs were fabricated with a configuration of ITO/HAT-CN (10 nm)/TAPC (45 nm)/Host: Flrpic (20 nm, 8 wt%)/TmPyPB (40 nm)/Liq (2 nm)/Al (120 nm), in which **pCzmOXD** or **mCzmOXD** acted as the phosphorescent host and Flrpic acted as the dopant.

PHOLEDs mentioned in this paper were fabricated through vacuum deposition of the materials at  $ca. 2 \times 10^{-6}$  Torr onto ITO-coated glass substrates. The ITO coated glass substrates were cleaned ultrasonically with acetone, ethanol, and deionized water, followed by dried in an oven, and exposed to UV-ozone for about



Scheme 2. Synthetic routes and chemical structures of **pCzmOXD** and **mCzmOXD**.

30 min. Organic materials, Liq and Al were deposited in the above sequence at a rate of 2–3 Å/s, 0.2 Å/s and 4 Å/s, respectively, through a shadow mask without breaking the vacuum between each deposition process. After cathode deposition the devices were encapsulated with a glass lid.

The EL spectra, CIE coordinates and  $J$ – $V$ – $L$  curves of the devices were measured with a PHOTO RESEARCH SpectraScan PR 655 photometer and a KEITHLEY 2400 SourceMeter constant current source at room temperature. The external quantum efficiency (EQE) values were calculated according to the previously reported methods.

### 3. Results and discussion

#### 3.1. Synthesis and characterization

The synthetic routes of **pCzmOXD** and **mCzmOXD** are outlined in Scheme 2. For both **pCzmOXD** and **mCzmOXD**, the 1,2,4-oxadiazole rings are formed from the corresponding amidoximes and acylchlorides. Due to the *para*-positions of the two phenyl rings adjacent to the 1,2,4-oxadiazole rings are activated by the inductive effect of the electron-withdrawing group, **pCzmOXD** was synthesized via aromatic nucleophilic substitution reaction between carbazole and the fluoro-1,2,4-oxadiazole in absence of any palladium catalyst. But for **mCzmOXD**, the fluorine at *meta*-position of the phenyl ring cannot be effectively activated and the reaction yield is quite low under the same condition as **pCzmOXD**. Thereby, we chose bromo-1,2,4-oxadiazole as the precursor to react with carbazole via Buchwald–Hartwig reaction to afford **mCzmOXD** in good yield. The molecular structures of the precursors and final products were confirmed by NMR spectroscopy, mass spectrometry, and elementary analyses.

#### 3.2. Morphology stability

Good morphological stabilities of materials are important for OLEDs, since the high  $T_g$  and thermal stability could withstand inevitable Joule heat encountered during device operation. To confirm their morphological stabilities, **pCzmOXD** and **mCzmOXD** were investigated by differential scanning calorimetry (DSC) under a nitrogen atmosphere at a scanning rate of 10 °C/min. As shown in Fig. 1, both materials presented glass transition above 100 °C, indicating better stability than the common used blue host material

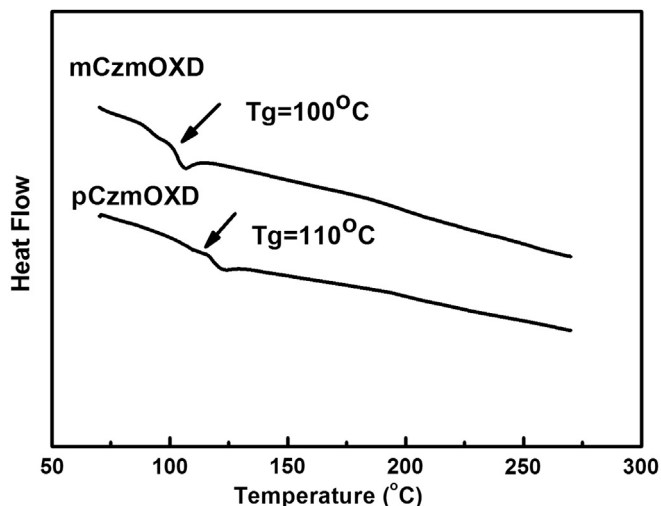


Fig. 1. DSC traces recorded at a heating rate of 10 °C/min.

**Table 1**  
Physical Properties of **pCzmOXD** and **mCzmOXD**.

Compound	$T_g^a$ [°C]	$\lambda_{\max, \text{abs}}^b$ [nm]		$\lambda_{\max, \text{em}}^b$ [nm]		HOMO/LUMO <sup>e</sup> [eV]		$E_T^d$ [eV]		$E_g^c$ [eV]
		exp	cal	exp	cal	exp	cal	exp	cal	
<b>pCzmOXD</b>	110	292, 341	440	5.98/2.72	5.42/1.89	2.71	2.69	3.24		
<b>mCzmOXD</b>	100	291, 337	451	5.99/2.47	5.38/1.94	2.81	2.88	3.52		

<sup>a</sup>  $T_g$ : glass transition temperatures.

<sup>b</sup> Measured in dichloromethane solution at room temperature.

<sup>c</sup>  $E_g$ : The band gap energies were estimated from the optical absorption edges of UV–Vis absorption spectra.

<sup>d</sup>  $E_T$ : The triplet energies were estimated from the onset peak of the phosphorescence spectra which were measured in 2-MeTHF glass matrix at 77 K.

<sup>e</sup> HOMO levels were calculated from CV data, LUMO levels were calculated from HOMO and  $E_g$ .

mCP. Therefore the two compounds can be used as stable organic materials for OLEDs under vacuum evaporation.

#### 3.3. Photophysical properties

The photophysical properties of **pCzmOXD** and **mCzmOXD** were investigated by electronic absorption and photoluminescence (PL) measurements at room temperature in  $\text{CH}_2\text{Cl}_2$ . The pertinent data are summarized in Table 1. The absorption and emission spectra of these two molecules are shown in Fig. 2. The absorption bands observed at about 250 and 296 nm of the two compounds are assigned to carbazole central transitions. The absorption in the range of 315 nm–352 nm could be attributed to the intramolecular charge transfer (ICT)  $\pi$ – $\pi^*$  transition from the electron-donating

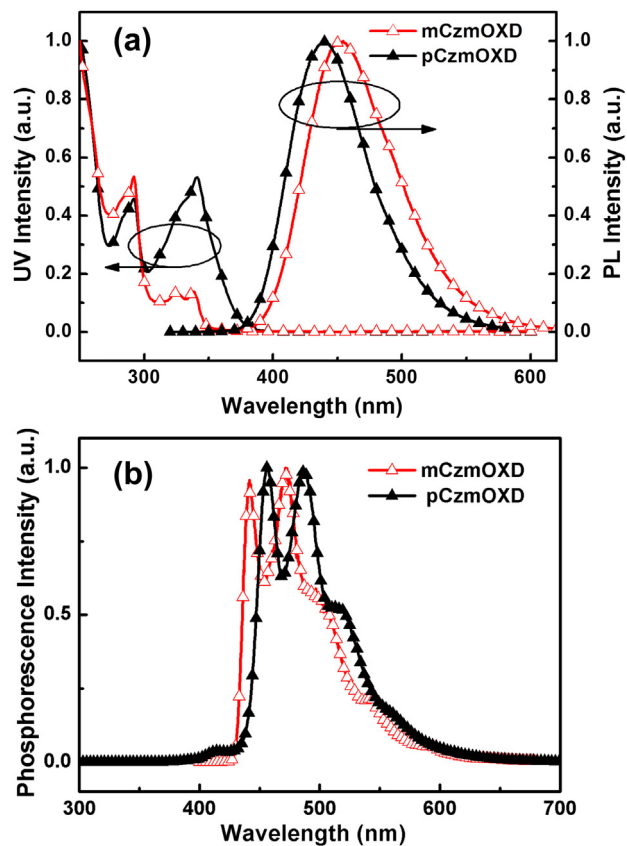


Fig. 2. (a) UV–Vis absorption and PL spectra of **pCzmOXD** and **mCzmOXD** in dichloromethane solution at  $10^{-5}$  M. (b) Phosphorescence spectra of **pCzmOXD** and **mCzmOXD** measured in a frozen 2-methyltetrahydrofuran matrix at 77 K.

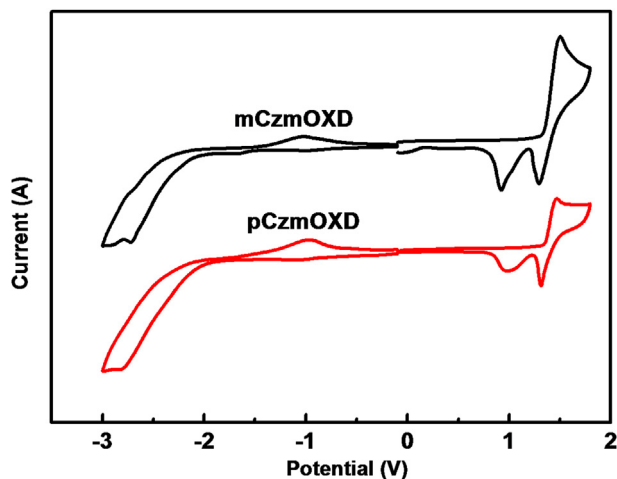


Fig. 3. Cyclic voltammograms in  $\text{CH}_2\text{Cl}_2$  for oxidation and DMF for reduction.

carbazole moiety to the electron-withdrawing 1,2,4-oxadiazole moiety in the backbone. It is clearly that the relative intensity of *para*-analogue is higher than that of *meta*-analogue, reflecting the larger transition dipole moment for the more effectively conjugation. Their energy gaps ( $E_g$ ), calculated from the threshold of the absorption spectra, are 3.24 and 3.52 eV for **pCzmOXD** and **mCzmOXD**, respectively. It is not beyond the expectation that the *meta* analogue should possess higher  $E_g$ , on the other hand, the emission spectra of **mCzmOXD** (max at 440 nm) show a red-shift relative to **pCzmOXD** (max at 450 nm), which is inconsistent with their absorption. The larger Stokes shift of **mCzmOXD** can be understood by their HOMO–LUMO distributions: the HOMO–LUMO separation in **mCzmOXD** is larger, indicating a larger charge separation and a more polar excited state, which will lead to larger Stokes shift in solvent (see *theoretical calculation* section). The phosphorescence of the two molecules was measured in 2-MeTHF glass at 77 K and the spectra of **pCzmOXD** and **mCzmOXD** are shown in Fig. 2. Their triplet energies ( $E_T$ ) are determined to be 2.71 and 2.81 eV for **pCzmOXD** and **mCzmOXD**, respectively, evaluated from the first phosphorescent emission peak. The  $E_T$  of **mCzmOXD** is evidently higher than that of **pCzmOXD** and is also higher than that of the common blue phosphorescent dopant Flrpic (2.62 eV). The higher  $E_T$  can be attributed to *meta*-linkage for **mCzmOXD**

instead of *para*-linkage in **pCzmOXD**. At the same time, the higher  $E_T$  of **pCzmOXD** and **mCzmOXD** than the corresponding 1,3,4-oxadiazole derivatives **p-CzOXD** and **m-CzOXD** (2.60 eV and 2.72 eV as mentioned in the previous work [34]) can be explained by the conjugation interruption effect of the *meta*-linkage method in 1,2,4-oxadiazole. Hence, we surmise **mCzmOXD** can be used as potential host for blue PHOLEDs.

### 3.4. Electrochemical properties

The electrochemical properties of the compounds were determined by cyclic voltammetry (CV) (Fig. 3). The two materials underwent oxidation and reduction to approximate the formation of stable cation and anion radicals, which suggests their bipolar transporting properties. The ionization potential (which corresponds to the HOMO level) of **pCzmOXD** and **mCzmOXD** were estimated from the onset of oxidation potentials as  $-5.98$  eV and  $-5.99$  eV, respectively. Their optical energy bandgaps ( $E_g$ ) were determined from the onset of the UV–Vis absorption in  $\text{CH}_2\text{Cl}_2$  solution. The electron affinity (corresponding to the LUMO level) of **pCzmOXD** and **mCzmOXD** were 2.72 eV and 2.47 eV, respectively, which calculated by subtracting the gap energy from the ionization potential. All the electronic data are summarized in Table 1.

### 3.5. Theoretical calculations

To further understand the structure–property relationship of the compounds, the electronic properties of the compounds were studied using density functional theory (DFT) and time-dependent DFT (TDDFT) calculations with the B3LYP hybrid functional.

Fig. 4 shows the HOMO and LUMO distributions of **mCzmOXD** and **pCzmOXD**. For the two compounds, the HOMO and LUMO distributions were quite the same, except the HOMO and LUMO of **mCzmOXD** were more localized than that of **pCzmOXD** which could be explained by the worse conjugation of *meta*-linkage compared with *para*-linkage. The separation between the HOMO and LUMO levels bring benefits to the efficient charge-carrier transport and the prevention of reverse energy transfer. As compared with the molecular orbital distribution of **p-CzOXD** and **m-CzOXD** [34], the separation between the HOMO and LUMO levels of **pCzmOXD** and **mCzmOXD** are much obvious, indicating more effective bipolarity. Fig. 4 also shows that the asymmetry of

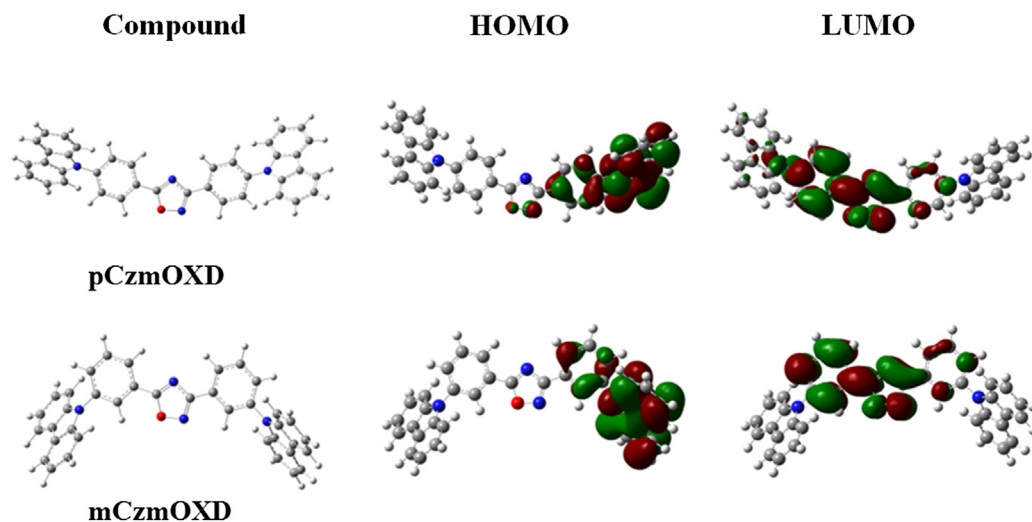


Fig. 4. Optimized geometry and HOMO–LUMO spatial distributions of **pCzmOXD** and **mCzmOXD**.

**Table 2**  
Electroluminescence characteristics of the devices.

Device	Host/guest	$V^a$ (V)	$\eta_c^b$ (cd A <sup>-1</sup> )	$\eta_p^b$ (lm W <sup>-1</sup> )	$\eta_{ext}^b$ (%)
A	pCzmOXD/Flrpic	4.54	13.0, 11.5, 9.9	10.7, 8.1, 4.4	5.6, 4.9, 4.2
B	mCzmOXD/Flrpic	3.35	16.0, 14.3, 9.9	16.8, 13.8, 5.9	6.8, 6.1, 4.2

<sup>a</sup> Voltage (V) at 100 cd m<sup>-2</sup>.

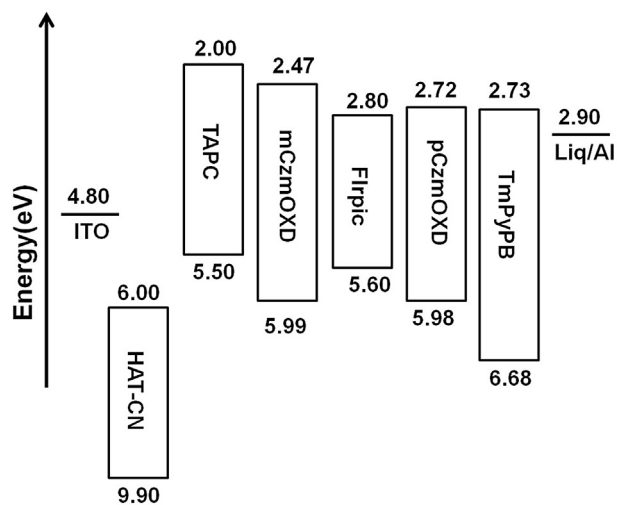
<sup>b</sup> Current efficiency ( $\eta_c$ ), power efficiency ( $\eta_p$ ) and external quantum efficiency ( $\eta_{ext}$ ) in the order of maximum, at 100 cd m<sup>-2</sup> and at 1000 cd m<sup>-2</sup>.

the 1,2,4-oxadizole can influence the distribution of the molecular orbitals, and the specific research is under study.

### 3.6. Electroluminescent properties

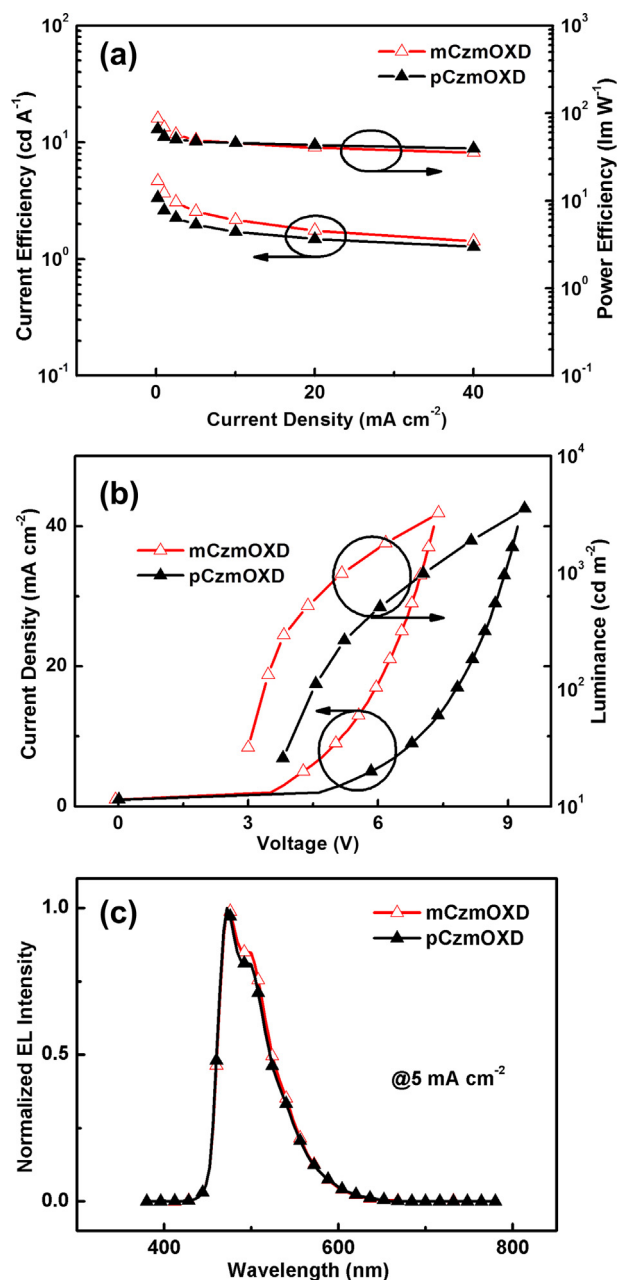
To assess the capability of pCzmOXD and mCzmOXD as bipolar host materials in PHOLEDs, a typical structure consisting of multiple organic layers sandwiched electrophosphorescent devices were fabricated. Due to the comparably high  $E_T$ , sky blue phosphorescent devices were fabricated using Ir-complex Flrpic doped into the hosts as emitting layer. Strongly electron-deficient 1,4,5,8,9,11-hexaazatriphenylene-hexacarbonitrile (HAT-CN) was deposited onto the precleaned ITO substrate to form the hole-injection layer (HIL). The 1,1-bis[4-[N,N-di(p-tolyl)amino]phenyl]cyclohexane (TAPC) served as the hole transport layer (HTL) and electron blocking layer (EBL). 1,3,5-tri[(3-pyridyl)-phen-3-yl]benzene (TmPyPB) was utilized as an exciton- and hole-blocking layer (HBL) for suppressing the blue excitons quenching at the emitting layer (EML)/electron-transporting layer (ETL) interface. Liq served as electron-injecting layer (EIL) and Al was utilized as cathode. These PHOLEDs have the configuration of ITO/HAT-CN (10 nm)/TAPC (45 nm)/Host: Flrpic (20 nm, 8 wt%)/TmPyPB (40 nm)/Liq (2 nm)/Al (120 nm) (Host = pCzmOXD: device A; Host = mCzmOXD: device B). The key parameters were summarized in Table 2. The schematic energy level diagrams of the two devices are shown in Fig. 5.

Fig. 6 depicts the current density–voltage–luminance ( $J$ – $V$ – $L$ ) characteristics, devices efficiency and EL spectra of the sky blue devices. Table 2 summarized the detail electroluminescence (EL) data. As shown in Fig. 6, both pCzmOXD and mCzmOXD based devices have low operating voltages of 4.54 and 3.35 V at a brightness of 100 cd m<sup>-2</sup>, which could be attributed to the ambipolar transporting property and the suitable HOMO and LUMO energy levels of the two compounds. The two devices exhibited



**Fig. 5.** Energy level diagrams for devices.

identical spectra with a peak at 476 nm and a shoulder at 500 nm, which was arisen from the typical emission of the phosphor Flrpic. As shown in Fig. 6 and Table 2, the mCzmOXD-based device has a maximum current efficiency (CE) of 16.0 cd A<sup>-1</sup>, a power efficiency (PE) of 16.8 lm W<sup>-1</sup> and an external quantum efficiency (EQE) of 6.8%. Obviously, the efficiency of the pCzmOXD-based device is lower than that of the mCzmOXD-based device. This fact can be explained by considering in the differences of both  $E_T$  and LUMO energy level between the two compounds. As mentioned before,  $E_T$  of pCzmOXD and mCzmOXD are 2.71 and 2.81 eV respectively, the higher  $E_T$  of mCzmOXD that could confine more triplet excitons within the emitting layers led to the higher device performance in mCzmOXD-based device. On the other hand, the LUMO energy level of mCzmOXD was estimated as  $-2.47$  eV, which is higher than



**Fig. 6.** (a) Current density–voltage–luminance characteristics; (b) current efficiency and power efficiency versus current density curves; (c) the EL spectra of devices at 5 mA cm<sup>-2</sup>.

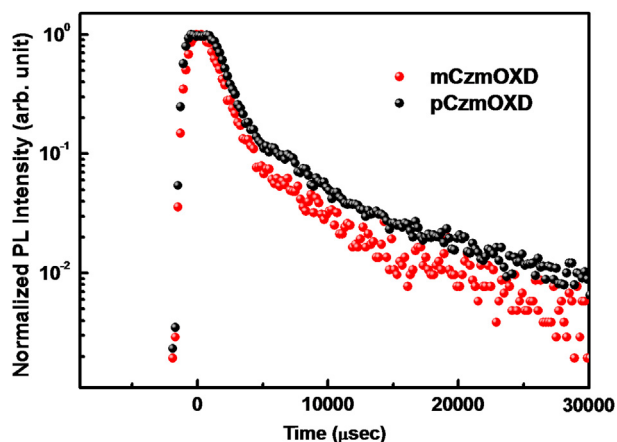


Fig. 7. Transient photoluminescence decay (excited at 330 nm) curves at room temperature at 472 nm for thin films of 10 wt% FIrpic co-deposited with **pCzmOXD** and **mCzmOXD**.

that of **pCzmOXD** (−2.72 eV), indicating that when used as host materials **mCzmOXD** could enhance electron trapping on the FIrpic, which can lead to direct charge recombination in the dopant. But for **pCzmOXD**, the LUMO energy level of **pCzmOXD** is close to FIrpic, indicating FIrpic could possibly emit through host-to-dopant energy transfer, which could introduce an intrinsic exchange energy loss derived from host-dopant energy transfer process. As a result, the device performance of **mCzmOXD**-based device is better than that of **pCzmOXD**-based device.

To further evaluate the effect of triplet energy difference on the device performance, transient photoluminescence decays of thin films (formed on quartz substrates with a thickness of 40 nm) with 10 wt% FIrpic dispersed in **mCzmOXD** and **pCzmOXD** were measured. The transient decays were fitted by biexponential equation. As depicted in Fig. 7, both the FIrpic-doped **mCzmOXD** and **pCzmOXD** films exhibit biexponential decay curves with long lifetimes of 1.67 and 2.01  $\mu\text{s}$ , respectively, which indicate the possibility of triplet energy transfer from FIrpic to **mCzmOXD** or **pCzmOXD** in the emissive layer. Obviously, **pCzmOXD**:FIrpic film exhibited a longer lifetime than **mCzmOXD**:FIrpic film, and this can be explained by the relatively high triplet energy level of **mCzmOXD** (2.81 eV), which can successfully suppress triplet energy back transfer from FIrpic to **mCzmOXD** in emission layer and well confine the triplet excitons on FIrpic, consequently resulting in efficient blue electrophosphorescence for **mCzmOXD** based device.

#### 4. Conclusions

In summary, we firstly developed one of the oxadiazole isomer-1,2,4-oxadiazole-in designing optoelectronic materials. Bipolar host materials **pCzmOXD** and **mCzmOXD** with this new electron-withdrawing block were synthesized and fully characterized. Incorporation of the 1,2,4-oxadiazole moiety could raise the triplet energies of **pCzmOXD** and **mCzmOXD** to 2.71 and 2.81 eV which allow the materials used in blue PHOLED. Good performance with low operating voltage and maximum current efficiency of 16.0  $\text{cd A}^{-1}$  are achieved, indicating that the 1,2,4-oxadiazole moiety used in OLED host materials is promising for further investigations.

#### Acknowledgments

We acknowledge financial support from the Natural Science Foundation of China (Nos. 21202114, 21161160446, 61036009, and 61177016), the National High-Tech Research Development Program

(No. 2011AA03A110), and the Natural Science Foundation of Jiangsu Province (No. BK2010003). This is also a project supported by Priority Academic Program Development of Jiangsu Higher Education Institutions (PAPD), and by the Fund for Excellent Creative Research Teams of Jiangsu Higher Education Institutions.

#### References

- [1] Tokuhisa H, Era M, Tsutsui T, Saito S. Electron drift mobility of oxadiazole derivatives doped in polycarbonate. *Appl Phys Lett* 1995;66:3433–5.
- [2] Tamoto N, Adachi C, Nagai K. Electroluminescence of 1,3,4-oxadiazole and triphenylamine-containing molecules as an emitter in organic multilayer light emitting diodes. *Chem Mater* 1997;9:1077–85.
- [3] Antoniadis H, Inbasekaran M, Woo EP. Blue-green organic light-emitting diodes based on fluorene-oxadiazole compounds. *Appl Phys Lett* 1998;73:3055–7.
- [4] Huang W, Meng H, Yu W-L, Gao J, Heeger AJ. A new blue light-emitting polymer containing substituted thiophene and an arylene-1,3,4-oxadiazole moiety. *Adv Mater* 1998;10:593–6.
- [5] Romeo G, Chiacchio U. Oxadiazoles. *Modern heterocyclic chemistry*. Wiley-VCH Verlag GmbH & Co. KGaA; 2011. p. 1047–252.
- [6] Jiang J-M, Yang P-A, Lan S-C, Yu C-M, Wei K-H. Benzooxadiazole-based donor/acceptor copolymers imparting bulk-heterojunction solar cells with high open-circuit voltages. *Polymer* 2013;54:155–61.
- [7] Bijleveld JC, Shahid M, Gilot J, Wienk MM, Janssen RAJ. Copolymers of cyclopentadithiophene and electron-deficient aromatic units designed for photovoltaic applications. *Adv Funct Mater* 2009;19:3262–70.
- [8] Ding P, Zhong C, Zou Y, Pan C, Wu H, Cao Y. 5,6-Bis(decyloxy)-2,1,3-benzooxadiazole-based polymers with different electron donors for bulk-heterojunction solar cells. *J Phys Chem C* 2011;115:16211–9.
- [9] Jiang J-M, Yang P-A, Chen H-C, Wei K-H. Synthesis, characterization, and photovoltaic properties of a low-bandgap copolymer based on 2,1,3-benzooxadiazole. *Chem Commun* 2011;47:8877–9.
- [10] Zhang Y, Zuniga C, Kim S-J, Cai D, Barlow S, Salman S, et al. Polymers with carbazole-oxadiazole side chains as ambipolar hosts for phosphorescent light-emitting diodes. *Chem Mater* 2011;23:4002–15.
- [11] Linton KE, Fisher AL, Pearson C, Fox MA, Palsson L-O, Bryce MR, et al. Colour tuning of blue electroluminescence using bipolar carbazole-oxadiazole molecules in single-active-layer organic light emitting devices (OLEDs). *J Mater Chem* 2012;22:11816–25.
- [12] Leung M-k, Yang W-H, Chuang C-N, Lee J-H, Lin C-F, Wei M-K, et al. 1,3,4-Oxadiazole containing silanes as novel hosts for blue phosphorescent organic light emitting diodes. *Org Lett* 2012;14:4986–9.
- [13] Lee J, Shizu K, Tanaka H, Nomura H, Yasuda T, Adachi C. Oxadiazole- and triazole-based highly-efficient thermally activated delayed fluorescence emitters for organic light-emitting diodes. *J Mater Chem C* 2013;1:4599–604.
- [14] Cheng S-H, Chou S-H, Hung W-Y, You H-W, Chen Y-M, Chaskar A, et al. Fine-tuning the balance between carbazole and oxadiazole units in bipolar hosts to realize highly efficient green PhOLEDs. *Org Electron* 2013;14:1086–93.
- [15] Ritchie J, Crayston JA, Markham JJP, Samuel IDW. Effect of meta-linkages on the photoluminescence and electroluminescence properties of light-emitting polyfluorene alternating copolymers. *J Mater Chem* 2006;16:1651–6.
- [16] Wang Q, Wallace JU, Lee TYH, Ou JJ, Tsai Y-T, Huang Y-H, et al. Evaluation of propylene-, meta-, and para-linked triazine and tert-butyltriphenylamine as bipolar hosts for phosphorescent organic light-emitting diodes. *J Mater Chem C* 2013;1:2224–32.
- [17] Cui L-S, Dong S-C, Liu Y, Xu M-F, Li Q, Jiang Z-Q, et al. meta-Linked spirobi-fluorene/phosphine oxide hybrids as host materials for deep blue phosphorescent organic light-emitting diodes. *Org Electron* 2013;14:1924–30.
- [18] Liu J, Li L, Gong C, Yu Z, Pei Q. An ambipolar poly(meta-phenylene) copolymer with high triplet energy to host blue and green electrophosphorescence. *J Mater Chem* 2011;11:9772–7.
- [19] Wu C, Tao S, Chen M, Mo H-W, Ng TW, Liu X, et al. A new multifunctional fluorenyl carbazole hybrid for high performance deep blue fluorescence, orange phosphorescent host and fluorescence/phosphorescence white OLEDs. *Dye Pigments* 2013;97:273–7.
- [20] Oh CS, Lee CW, Lee JY. A diphenyl ether bridged, high triplet energy host material for blue phosphorescent organic light-emitting diodes. *Dye Pigments* 2013;98:372–6.
- [21] Jiang W, Duan L, Qiao J, Dong G, Zhang D, Wang L, et al. Novel carbazole/pyridine-based host material for solution-processed blue phosphorescent organic light-emitting devices. *Dye Pigments* 2012;92:891–6.
- [22] Han C, Xie G, Xu H, Zhang Z, Yan P, Zhao Y, et al. Xanthene-based phosphine oxide host with the planar multi-insulating structure for efficient electrophosphorescence. *Dye Pigments* 2012;94:561–9.
- [23] Xiao L, Chen Z, Qu B, Luo J, Kong S, Gong Q, et al. Recent progresses on materials for electrophosphorescent organic light-emitting devices. *Adv Mater* 2010;23:926–52.
- [24] Tao Y, Yang C, Qin J. Organic host materials for phosphorescent organic light-emitting diodes. *Chem Soc Rev* 2011;40:2943–70.
- [25] Dong S-C, Gao C-H, Zhang Z-H, Jiang Z-Q, Lee S-T, Liao LS. A new Dibenzofuran/spirobi-fluorene hybrids as thermally stable host materials for efficient

- phosphorescent organic light-emitting diodes with low efficiency roll-off. *Phys Chem Chem Phys* 2012;14:14224–8.
- [26] Dong S-C, Gao C-H, Yuan X-D, Cui L-S, Jiang Z-Q, Lee S-T, et al. Novel dibenzothioophene based host materials incorporating spirobifluorene for high-efficiency white phosphorescent organic light-emitting diodes. *Org Electron* 2013;14:902–8.
- [27] Cui L-S, Dong S-C, Liu Y, Li Q, Jiang Z-Q, Liao L-S. A simple systematic design of phenylcarbazole derivatives for host materials to high-efficiency phosphorescent organic light-emitting diodes. *J Mater Chem C* 2013;1:3967–75.
- [28] Tao Y, Wang Q, Ao L, Zhong C, Qin J, Yang C, et al. Molecular design of host materials based on triphenylamine/oxadiazole hybrids for excellent deep-red phosphorescent organic light-emitting diodes. *J Mater Chem* 2010;20:1759–65.
- [29] Tao Y, Wang Q, Yang C, Zhang K, Wang Q, Zou T, et al. Solution-processable highly efficient yellow- and red-emitting phosphorescent organic light emitting devices from a small molecule bipolar host and iridium complexes. *J Mater Chem* 2008;18:4091–6.
- [30] Tao Y, Wang Q, Yang C, Wang Q, Zhang Z, Zou T, et al. A simple carbazole/oxadiazole hybrid molecule: an excellent bipolar host for green and red phosphorescent OLEDs. *Angew Chem Int Ed* 2008;47:8104–7.
- [31] Han C, Zhang Z, Xu H, Yue S, Li J, Yan P, et al. Short-axis substitution approach selectively optimizes electrical properties of dibenzothioophene-based phosphine oxide hosts. *J Am Chem Soc* 2012;134:19179–88.
- [32] Han C, Xie G, Xu H, Zhang Z, Xie L, Zhao Y, et al. A single phosphine oxide host for high-efficiency white organic light-emitting diodes with extremely low operating voltages and reduced efficiency roll-off. *Adv Mater* 2011;23:2491–6.
- [33] Chaskar A, Chen H-F, Wong K-T. Bipolar host materials: a chemical approach for highly efficient electrophosphorescent devices. *Adv Mater* 2011;23:3876–95.
- [34] Tao Y, Wang Q, Yang C, Zhong C, Zhang K, Qin J, et al. Tuning the optoelectronic properties of carbazole/oxadiazole hybrids through linkage modes: hosts for highly efficient green electro phosphorescence. *Adv Funct Mater* 2010;20:304–11.